Computational Model for Calculating Body-core Temperature Elevation in Rabbits Due to Whole-body Exposure at 2.45 GHz

Akimasa Hirata[1], Hironori Sugiyama[1], Masami Kojima[2], Hiroki Kawai[3], Yoko Yamashiro[2], Osamu Fujiwara[1], Soichi Watanabe[3], and Kazuyuki Sasaki[2]

1: Nagoya Institute of Technology, Japan

2: Kanazawa Medical University, Kanazawa, Japan

3: National Institute of Information and Communications Technology, Tokyo, Japan

Abstract

In the current international guidelines and standards with regard to human exposure to electromagnetic waves, the basic restriction is defined in terms of the whole-body average specific absorption rate. The rationale for the guidelines is that the characteristic pattern of thermoregulatory response is observed for the whole-body average SAR above a certain level. However, the relationship between energy absorption and temperature elevation were not well quantified. In this study, we improved our thermal computation model for rabbits, which was developed for localized exposure on the eye, in order to investigate the body-core temperature elevation due to whole-body exposure at 2.45 GHz. The effect of anesthesia on the body-core temperature elevation was also discussed in comparison with measured results. For the whole-body average SAR of 3.0 W/kg, the body-core temperature in rabbits elevates with time, without becoming saturated. The administration of anesthesia suppressed body-core temperature elevation, which is attributed to reduced basal metabolic rate.

Keywords Microwave exposure, body-core temperature rise, whole-body averaged SAR, bio-heat equation

1. Introduction

There has been increasing public concern about the adverse health effects of human exposure to electromagnetic waves. In the radio-frequency and microwave (MW) regions, elevated temperature (1-2^{o}C) resulting from energy absorption is known to be a dominant factor inducing adverse health effects such as heat exhaustion and heat stroke (ACGIH 1996). In safety standard and associated documents in 1980s (ANSI 1982, Elder and Cachill 1983), the whole-body average specific absorption rate (SAR) was used as a measure of human protection for MW whole-body exposure. The threshold whole-body average SAR is 4-8 W/kg in the ANSI (American National Standards Institute) standard (1982) and 1-2 W/kg in the review by the EPA (Environmental Protection Agency) (Elder and Cachill 1983). These thresholds are based on the fact that MW exposure of laboratory animals in excess of approximately 4 W/kg has revealed a characteristic pattern of thermoregulatory response (Michaelson 1983). In addition, decreased task performance by rats and monkeys has been observed at SAR values in the range of 1–3 W/kg (Stern et al 1979, Adair and Adams 1980, D'Andrea 1986). Because the physiological heat loss mechanisms are limited, however, these small animals would be poor models for human beings (Adair and Black 2003).

Even in the current international guidelines and standards (ICNIRP 1998, IEEE 2006), the basic restriction is defined in terms of whole-body average SAR, as is the same in the standard in the 1980s (ANSI 1982, Elder and Cachill 1983). Its limit is 0.4 W/kg for occupational exposure. According to the ICNIRP guidelines (1998), the rationale of this limit is that human exposure for less than 30 min. caused a body-core temperature elevation of less than 1 ^{o}C under the conditions in which the whole-body average SAR was less than 4 W/kg. Then, a safety factor of 10 has been applied to the above value to provide adequate human protection. Only limited cases, especially for partial-body exposures, were considered in these studies: i) localized exposure to the legs (Hoque and Gandhi 1988) and ii) clinical data for magnetic resonance imaging (Shellock and Crues 1987), e.g.

The animal studies for the whole-body exposures referenced in the international guidelines were conducted in the 1970s and 80s (Adair and Adams 1980, Stern et al 1979, Michaelson 1983). Although a characteristic pattern of thermoregulatory response was observed in animals, body-core temperature elevation due to MW energy was not quantified. The main reason for this is that until recently experimental and computational dosimetric techniques were not well established. Ebert et al (2005) determined thermal regulatory and breakdown thresholds for mice with respect to whole-body average SAR. However, thermal analysis was not conducted, and no anesthesia was used in that study. Additionally, in these studies (Adair and Adams 1980, Stern et al 1979, Michaelson, 1983, Ebert et al 2005), laboratory rodents were employed. The effect of species on temperature elevation due to MW energy was not well investigated. Hirata

et al (2006) succeeded in developing a computational code for temperature variation in the rabbit eye for intense localized MW energy, considering body-core temperature variation. Thus, it is worth extending this computational code to examine the body-core temperature elevation for whole-body MW exposures.

The purpose of this study is to develop and validate the computational code for clarifying the relationship between incident electromagnetic fields, whole-body average SAR, and rectal temperature elevation in the rabbits. First, we retuned the thermal constants of rabbit tissues, which were validated for the dosimetry of localized exposure to the eye (Hirata *et al* 2006). As a far-field MW source, a double-ridged waveguide horn antenna was used. In the computation, a plane wave was considered for simplicity. The time courses of computed and measured temperature elevations are compared in order to validate our computational model. The effect of anesthesia on body-core temperature elevation was also discussed with comparison of the computational and measured results.

2. Model and Methods

2.1 Experimental Setup

In order to validate our computational model, we conducted an experiment. The rabbits used in this experiment were cared for and handled in accordance with the Guidelines for Animal Experiments at Kanazawa Medical University. The average weight of young adult male pigmented rabbits was 2.0 kg (±10%). During exposure, the pigmented rabbit was immobilized in a polycarbonate rabbit holder (Kojima *et al* 2004). In case without microwave exposures, the temperature variation due to rabbit insertion for 30 min or more in the holder was confirmed to be marginal. This would be because the heat transfer between air and skin is not dominant in the thermal balance of rabbits (Marai et al 2002).

The rabbit is exposed under anesthesia (ketamine hydrochloride (5 mg/kg)+ xylazine (0.23 mg/kg) injected intramuscularly) or without anesthesia in order to investigate the effect of anesthesia on the body-core temperature elevation. Note that the administration of anesthesia reduce the blood perfusion and basal metabolic rate together with inactivating thermoregulatory response (Adair et al 1984, Hirata et al 2006).

For measuring the body-core temperature (Kojima et al 2004), a flexible thermal probe (1.6 mm in diameter) was inserted 100 mm into the rectum. The Fluoroptic thermometer (Anritsu FL-2000, Tokyo, JAPAN) was calibrated using a standard thermometer. The resolution of the probe is 0.1 ^{o}C and measured at each 10 s.

Added to the rectal temperature, the eye temperature was measured in this study. In the thermal modeling, there are many thermal parameters. This simultaneous measurement at different points would validate our computational modeling definitely. The reason for choosing the lens is

that it is stable to fix the probe. In addition, the eye is located around the surface. The modeling around the eye for localized exposures is generally succeeded in our previous study (Hirata et al 2006).

Temperatures of the eye segments were measured with a Fluoroptic thermometer (Luxtron 790, Luxtron, Santa Clara, CA) according to the following procedures: each rabbit eye was anesthetized with a 0.4% oxybuprocaine hydrochloride ophthalmic solution applied as eye drops; thermometer probes (0.5 mm in diameter) were then inserted into the lens nuclear part. The tip of thermal probe was set on an optical axis in the center in the pupillary zone, and measured at each second. Room temperature was kept to 24-25 ^{o}C by an air conditioner.

As a MW source, a double-ridged waveguide horn antenna (ETS-LINDGREN Inc., Model 3115, ETS-LINDGREN, Cedar Park, TX) was used. The MW frequency was 2.45 GHz. A 1-m distance between rabbit and antenna was chosen so that fields radiated from the antenna are considered as far-fields. The signal generated in an electric signal generator (Agilent, E4438C-402, Agilent Technologies, Santa Clara, CA) was amplified via a power amplifier (BONN Elektronik Inc., TWAL 0208-250, BONN Elektronik, Ottobrunn, Germany). The power fed to the antenna was monitored with a power sensor (Agilent, 8481A) throughout the measurement in order to confirm that radiated power is kept constant to 140±6 W. The experimental setup is given in Fig. 1. Note that rabbits were irradiated from the lateral side to maximize the whole-body average SAR at the same incident power density.

Since we used the horn antenna, the radiated fields cannot be considered as a plane wave. In order to estimate effective power incident to a rabbit, we measured the electric field in the region of a rabbit using a probe with a resolution of 50 or 100 mm, as illustrated in Fig. 2. From our measurement, the corresponding average power density was 252 W/m^2 with a deviation of ±35%. This average power is expected to be reasonable since the reference levels in the ICNIRP guidelines (1998), which are field or power density for practical exposure assessment, are intended to be spatially averaged values over the entire body of the exposed individual.

2.2 Numeric Rabbit Phantom

We have developed an anatomically-based rabbit phantom with a resolution of 1 mm. This was constructed on the basis of X-ray CT images taken at Kanazawa Medical University, Japan (Wake et al 2007). This model is comprised of 12 tissues: skin, muscle, bone, fat, brain, CSF, anterior chamber, vitreous, retina/choroid/sclera, iris/ciliary body, lens, and cornea. Specifically, their thicknesses become largest around the optic nerve head. In our model, the retina/choroid/sclera is further classified into two parts on the basis of the blood perfusion. Further discussion on the tissue classification can be found in Hirata et al (2006). The width, depth, and height of this model were 123 mm, 260 mm, and 152 mm, respectively. The weight

of the rabbit phantom was 2.5 kg. In order to match the average weight of rabbits employed in this study and that of the phantom, we reduce linearly the cell size of the rabbit phantom from 1 mm to 0.93 mm.

2.3 SAR Calculation

The FDTD method (Taflove and Hagness 1995) is used for investigating MW power absorbed in the rabbit phantom. For a truncation of the computational region, we adopted perfectly matched layers as the absorbing boundary. To incorporate the rabbit model into the FDTD scheme, the dielectric properties of tissues were required. They were determined with the 4-Cole-Cole extrapolation (Gabriel 1996).

For harmonically varying fields, the SAR is defined as

$$\mathrm{SAR} = \frac{\sigma}{2\rho} |\hat{E}|^2 = \frac{\sigma}{2\rho}(|\hat{E}_x|^2 + |\hat{E}_y|^2 + |\hat{E}_z|^2) \quad (1)$$

where $\hat{E}_x$, $\hat{E}_y$, and $\hat{E}_z$ are the peak values of the electric field components, σ and ρ, denoting the conductivity and the mass density of the tissue, respectively.

2.4 Temperature Calculation

Our formula for the temperature calculation was given in our previous study (Hirata et al 2006). In that study, we applied an active blood perfusion model of human to rabbits (Hoque and Gandhi 1988), together with a parametric study. The sweat glands in rabbits are virtually nonfunctional, allowing us to neglect this mechanism in our modeling. During heat stress, rabbits try to sustain homeothermy using internal physiological measures (Marai et al 2002), such as changes in breathing rates and peripheral (ear) temperatures. In our measurement, the increased breathing rates, together with licking the nose, were observed. Although these responses were not fully taken into account in our modeling, the effect of these responses on the temperature elevation will be commented in Sec. 3.2.

2.4.1 Bioheat Equation

For calculating temperature increases in the rabbit model, the bioheat equation was used [23]:

$$C(\mathbf{r})\rho(\mathbf{r})\frac{\partial T(\mathbf{r},t)}{\partial t} = \nabla\cdot(K(\mathbf{r})\nabla T(\mathbf{r},t)) + \rho(\mathbf{r})SAR(\mathbf{r}) + A(\mathbf{r}) - B(\mathbf{r},t)(T(\mathbf{r},t) - T_B(t)) \quad (2)$$

where $T(\mathrm{r},t)$ and $T_B(t)$ denote the respective temperatures of tissue and blood, *C* the specific heat of tissue, *K* the thermal conductivity of tissue, *A* the basal metabolism per unit volume, and *B* the term associated with blood flow. The blood temperature is assumed to be

constant over the whole body, since the blood circulates throughout the human body in one minute or less. In rabbits, it takes far less time due to the smaller dimensions and higher blood perfusion rate than in human. The boundary condition between air and tissue for Eq. (2) is given by the following equation:

$$-K(r)\frac{\partial T(\mathbf{r},t)}{\partial n} = h\cdot(T_s(\mathbf{r},t)-T_e(t)) \qquad (3)$$

where H, T_s, and T_e denote, respectively, the heat transfer coefficient, surface temperature, and air temperature. The heat transfer coefficient h is given by the summation of radiative heat loss h_{rad}, convective heat loss h_{conv}, and evaporative heat loss h_e,.

The bioheat equation is particularly effective in the shallow region of the body where the vasculature system is not required to model (Wissler 1998). In other words, the temperature calculated becomes unreliable with the distance from the body surface. However, the microwave power absorption or heat source is concentrated around the surface at 2.45 GHz exposure system, since the penetration depth of the microwave is at a few centimeters. Therefore, the body-core temperature elevation would be mainly caused by the circulation of temperature-elevated blood. Therefore, the calculation scheme for the blood temperature is essential in this computational modeling. The temperature of blood is changed according to the following equation in order to satisfy the thermodynamic laws (Bernardi et al 2003, Hirata et al 2006, 2007):

$$T_B(t) = T_{B0} + \int_t \frac{Q_{BTOT}(t)}{C_B\rho_B V_B}dt \qquad (4)$$

$$Q_{BTOT}(t) = \int_V B(t)(T_B(t)-T(\mathbf{r},t))dV \qquad (5)$$

where Q_{BTOT} is the rate of heat acquisition of blood from body tissues. C_B (=4000 J/kg·^{o}C), ρ_B (=1050 kg/m^3), and V_B denote the specific heat, mass density, and total volume of blood, respectively. Note that the average blood volume per unit rabbit body mass is 56 ml/kg. The blood volume is put at 110 ml, since the weight of our rabbits averaged around 2.0 kg. It should be noted that Eq. (6) was introduced and substituted into Eq. (4) instead of Q_{BTOT} for evaluating the net rate of heat acquisition of blood from body tissues as follows:

$$Q_{BN}(t) = Q_{BTOT}(t) - Q_{BTOT}(0) \qquad (6)$$

Eq. (6) is necessary because Eq. (4) is not zero even at time t=0, which is attributed to some computational simplification or assumption, including a discretized anatomically-based model with finite resolution, uniform distribution of blood temperature over the body, and uncertainty in the basal metabolism of tissues depending on the individual and body parts.

2.4.2 Thermoregulatory responses

For a temperature elevation above a certain level, the blood perfusion was activated in order to

carry away the excess heat produced. As to blood perfusion for all tissues except the skin, the regulation mechanism was governed by the local tissue temperature. When that temperature remained below a certain level, blood perfusion was equal to its basal value B_0. Once the local temperature exceeded a given threshold, the blood perfusion increased almost linearly with the temperature in order to carry away the heat produced. For humans, these mechanisms are expressed by the following equations (Hoque and Gandhi 1988):

$$B(\mathbf{r},T(\mathbf{r})) = B_0(\mathbf{r}), \qquad T(\mathbf{r}) \le T_A \qquad (7)$$

$$B(\mathbf{r},T(\mathbf{r})) = B_0(\mathbf{r})\left(1+(\alpha-1)\frac{T(\mathbf{r})-T_A}{T_B-T_A}\right), \qquad T_A < T(\mathbf{r}) \le T_B \qquad (8)$$

$$B(\mathbf{r},T(\mathbf{r})) = \alpha B_0(\mathbf{r}), \qquad T(\mathbf{r}) > T_B \qquad (9)$$

where T_A [^{o}C] and T_B [^{o}C] denote the threshold temperatures at which the blood perfusion activates and saturates, respectively. The coefficient α must be larger than 1. For our parametric study on rabbit, it was found to be reasonable that T_A is initial rectal temperature, T_B- T_A=5 ^{o}C, and α=5 (Hirata et al 2006).

The variations of blood perfusion in the skin through vasodilatation are expressed in terms of the temperature increase in the hypothalamus $T_H - T_{H0}$ and the average temperature increase in the skin ΔT_S:

$$B(\mathbf{r},T(\mathbf{r},t)) = (B_0(\mathbf{r}) + F_{HB}(T_H(t) - T_{H0}) + F_{SB}\Delta T_S(t)) \cdot 2^{(T(\mathbf{r},t)-T_0(\mathbf{r}))/6} \qquad (10)$$

where

$$\Delta T_S(t) = \frac{\int_S (T(\mathbf{r},t) - T_0(r))dS}{S}. \qquad (11)$$

where T_0, F_{HB}, and F_{SB} are the steady-state temperature without heat load and the weighting coefficients of signal from the hypothalamus and skin, respectively. These values were taken from (Bernardi 2003).

In addition to these responses, the breathing rates were increased for the temperature elevation above a certain level. This change would influence the heat transfer coefficient between internal air and tissues. This coefficient will be determined in Sec. 3.1.

2.4.3 Thermal Constants of Tissues

Table 1 lists specific heat, thermal conductivity, basal metabolic rate, and the term associated with blood perfusion for rabbit tissues. The specific heat and thermal conductivity of tissues (Cooper and Trezek 1971) were extrapolated on the basis of their water content (ICRP 1975). The blood perfusion rate except for eye tissues were extrapolated from the data for sheep, rats, etc., together with the correlation between the body mass and the basal metabolic rate. The basal metabolic rate was estimated by assuming that it was proportional to the blood perfusion (Gordon et al 1976). For a more detailed discussion, see our previous study (Hirata et al 2006).

We used the heat transfer coefficient between the cornea and air from our previous study: $30\,W/m^2/^oC$ (Hirata et al 2006). Furthermore, the heat transfer coefficient between tissue and internal air was set at 55 $W/m^2/^oC$ (Taflove and Brodwin 1975). Heat transfer coefficients between the skin and the air and between the ear lobe and skin will be discussed in the next section.

3. Results

3.1 Computation of Heat Transfer Coefficients

We discussed the heat transfer coefficient between the skin and air. We subdivided the skin into two parts: ear lobe and the other parts. In Marai et al (2002), the average temperature of skin and ear lobe were reported to be 38.6 ^oC and 33.8 ^oC, respectively, at the air temperature of 25 ^oC. At that time, rectal temperature was 39.5 ^oC. For these values, we determined 0.65 $W/m^2\cdot{}^oC$ and 2.5 $W/m^2\cdot{}^oC$ as the respective values of the heat transfer coefficient between the skin and the air and between the ear lobe and the air. These values are equivalents including the effect of stair-casing approximation of numeric rabbit phantom. Therefore, the actual heat transfer coefficients would be larger than these values by a factor of 1.4 or less (Samaras et al 2006). Since it would influence our computational results marginally, we avoid further discussion on this problem. We estimated the heat transfer coefficient between skin and air as 2-3 $W/m^2/^oC$ by comparing measured and computed temperatures on the scalp (Hirata et al 2006). This value is higher than the value obtained in the present study. This difference would be caused by the blood temperature in the scalp which is lower than in the other parts. The blood temperature was assumed to be constant over the whole body in our calculation (see Eq. (1)).

3.2 Temperature Elevation in Unanesthetized and Anesthetized Rabbit

Immobilized rabbit was exposed to 2.45-GHz far-field energy radiated by the double-rigged antenna, as shown in Fig. 2. Two cases were considered: with and without anesthesia. Our measurements were conducted for five unanesthetized and six anesthetized rabbits. However, rabbits move slightly even in the plastic holder, resulting in unstable temperature evolution for both cases. Note that the resolution of temperature probe is 0.1 ^oC, and abrupt change in the temperature was 0.2 ^oC or more. Therefore, we will show the results for two rabbits without anesthesia and four rabbits with anesthesia whose time courses of the temperature elevation were stable. Then, the mean average values of temperatures over 20 sec. will be plotted in the following figures.

In the initial state, the rectal temperature for two rabbits without anesthesia was 40.2 ^oC, while that for five rabbits with anesthesia was in the range between 39.7 and 40.8 ^oC. MW exposures were terminated before rectal temperature elevation reaches 42 ^oC. Thus, the purpose

of this study is not to discuss the rabbit breakdown threshold but to discuss the relationship among the incident electromagnetic field, whole-body average SAR, and body-core temperature elevation.

Figure 3 illustrates the SAR distributions in the numeric rabbit phantom when exposed to 2.45-GHz plane wave with the power density of 252 W/m^2. The whole-body average SAR was 3.0 W/kg. High SAR is observed around the ear lobe. However, the total amount of power absorbed in the ear lobes was at most 3%, suggesting that the modeling around ear lobe is not essential. With this SAR distribution, we calculated the temperature elevation in the blood (or body core) and eye lens.

Figures 4 (a) and (b) show the time variation of blood temperature in case without and with anesthesia, respectively. In Fig. 4 (b), the calculation when neglecting the vasodilatation (neglecting temperature-dependent blood perfusion rate in rabbits, or not considering Eqs. (7)-(10)) is also shown. This is because the administration of anesthesia inactivates thermoregulatory response (Adair et al 1984, Kojima et al 2004). From Fig. 4(a), calculated and measured temperature elevations are in good agreement. Some abrupt changes were observed in measured temperatures due to the rabbit moving slightly in the holder, which also altered the probe position (Kojima et al 2004). After 1200 sec. (20 min.) passed, increased breathing rates with licking the nose were observed for the two rabbits. However, it is clear from the figure that this response does not work effectively to cool down the body. The rectal temperature at 1200 sec. was 41.4-41.5^{o}C. At 2000 sec. the rectal temperature reached 42 ^{o}C, and we then stopped our experiment. For the first few ten minutes, good reproducibility was obtained in the time course of the temperature elevation for other rabbits. From Fig. 4 (b), the measured rectal temperatures are generally smaller than that of calculation, since anesthesia is suggested to reduce the basal metabolism (Adair et al 1984, Hirata et al 2006). Note that anesthetic depth depends on individuals and body parts (Tuma et al 1981). For our measurements for five rabbits, the reduction of basal metabolism was in the range of 8-36% except for one sample.

Figures 5 (a) and (b) show the temperature in the lens with and without anesthesia. From Fig. 5 (a), good agreement is observed in the first 5 min, as well as that as the blood temperature. In the first several minutes, the temperature elevation is mainly caused by the EM power absorption. Some differences are observed over time. This would be caused by rectal or blood temperature. Elevated body-core or blood temperature elevates tissue temperature, as can be seen from Eq. (2).

4. Discussion

4.1 Heat Balance in Rabbits

Let us consider the heat balance given in Ebert et al (2005) based on Adair and Black (2003):

$$M + P_{RF} - P_{conv} = S \quad (12)$$

where M is the rate at which thermal energy is produced through metabolic processes, P_{RF} the RF power absorbed in the the body, P_{conv} the rate of heat exchange with the convection, and S the rate of heat storage in the body.

Increased breathing rates were observed in the rabbits without anesthesia, corresponding to the increase of the value P_{conv} in Eq. (12). For our computational fitting, the heat transfer coefficient between internal air and tissue increased by a factor of 3, or became 150 W/m^2/^{o}C. However, the increased value of P_{conv} would be marginal as compared with the other factors.

The basal metabolism in the rabbits with anesthesia is reduced (Tuma et al, 1981). From Eq. (12), the effect of reduced basal metabolism on the rate of heat storage is linear. Therefore, the effect of anesthesia can be included in our computational code by simply reducing the basal metabolism by 5-35%, based on our measurement. The reduction of basal metabolism was confirmed in the rabbits without microwave exposures. Note that the measured body-core temperature elevation was larger than calculated ones for the one sample of exception. The reason for this is not clear, but we suppose that it is caused by the increased basal metabolism due to increased rabbit tension when the anesthetic depth becomes shallower with time.

No clear difference was observed between calculated temperatures with and without the thermoregulatory response in the rabbit with anesthesia. This marginal difference is because the blood perfusion rate does not significantly influence the heat balance between rabbit and air significantly, as is evident from Eq. (12). Namely, this marginal difference is caused by the change in the blood perfusion rate or different skin temperature, leading to a small difference in heat transfer between air and skin (Eq. (3)).

4.2 Temperature Elevation in the Eye with Revised Thermal Parameters

The thermal parameters in the present study were revised from those in our previous study (Hirata et al 2006). In the present study, there were some differences between computed and measured temperatures in the lens. In order to discuss the reason for this difference, we applied the revised thermal parameters to the condition for localized exposure in Hirata et al (2006). The difference of temperature in the lens with original and revised parameters was less than 3%.

As shown in Fig. 5, measured and computed temperatures in the first several minutes were in good agreement in case with and without anesthesia, while some differences were observed with time. From comparison between Figs. 5 (a) and (b), the measured temperature with anesthesia is closer to the computed one than that without anesthesia. Note that thermoregulatory response is inactivated for rabbits with anesthesia. Thus, the difference between measured and computed

temperatures would be caused by the rabbit thermophysiology, such as the tears and a blink of the eye. The time course of the samples of 6 and 7 are in good agreement with the computed results till 1200 sec. The duration of anesthesia is generally less than 30 minutes. Therefore, the difference after 1200 sec. is considered to be caused by anesthetic depth.

The effect of anesthesia on the computed temperature elevations in the lens was marginal from Fig. 5 (b), unlike in Hirata et al (2006). This is because the temperature elevation even in the lens or at the shallow region is at most 1.5 ^{o}C, which is much smaller than the 6 ^{o}C or so which was observed for localized exposures. Namely, thermoregulatory response works marginally for whole-body exposures.

4.3 Comparison with Previous studies on rodents and humans

For the whole-body average SAR of 3.0 W/kg, the body-core temperature in rabbits elevates with time, without getting saturated. This SAR value is much smaller than that of mice determined by Ebert et al (2005): whole-body average SARs of thermal regulatory and breakdown thresholds for mice were 2-5 W/kg and 6-14 W/kg, respectively, for 2 *h* exposure. This difference would be because of the weak susceptibility of rabbits to heat stress (Marai et al 2002), in addition to the difference in the basal metabolism (Ebert et al 2005).

The calculated whole-body average SARs required to elevate body-core temperature elevation in a rabbit by 1 ^{o}C were 2.3 and 1.3 W/kg for 30 min. and 1 h, respectively, against 6.7 and 6.5 W/kg for human (Hirata et al 2007). The temperature elevation in a human became saturated within a half hour or so, since the heat can become balanced in a human due to sweating, unlike a rabbit. These comparisons support the notion that the human has a thermoregulatory ability greater than other endotherms during RF exposure (Adair and Black 2003).

4. Summary

In the current international guidelines and standards (ICNIRP 1998, IEEE 2006), the basic restriction is defined in terms of whole-body average SAR. In addition to the human studies, animal studies especially on rodents were referenced in these guidelines and standards. The rationale for the guidelines is that a characteristic pattern of thermoregulatory response is observed for the whole-body average SAR above a certain level. However, the relationship between energy absorption and temperature elevation were not stated in detail. The relationship in animals is highly useful to extrapolate the human, or helpful to confirm the scientific basis of current safety guidelines for human protection.

In this study, we improved our thermal computation model for rabbits, which was developed for localized exposure, to consider the body-core temperature elevation due to whole-body exposure at 2.45 GHz. The effect of anesthesia on the body-core temperature elevation was also

discussed with the computational code developed in this study.

For the whole-body average SAR of 3.0 W/kg, the body-core temperature in rabbits elevates with time, without becoming saturated. The time course of body-core temperature was different from mice (Ebert et al 2005) and humans (Hirata et al 2007). The main reason for this difference would be the thermoregulatory response. The administration of anesthesia suppressed body-core temperature elevation, which is attributed to reduced basal metabolic rate. When reviewing the findings in animal studies and then extrapolating to humans, the difference in the thermophysiology and the administration of anesthesia should be considered.

For lower MW power density than used in this study, we found that the body-core temperature elevation in rabbits with anesthesia becomes comparable to the temperature decrease due to the reduction of basal metabolism. In addition, the duration of anesthesia is generally less than 30 minutes, and thus we could not investigate the temperature elevation for lower MW power density. This new computational model would be helpful to design experiments. In future, we plan to investigate experimentally the dependence of body-core temperature elevation in rabbit on MW power absorption conditions, i.e., strength and duration, as Ebert et al (2003) did in mice.

Acknowledgement

This study was supported in part by the International Communications Foundations, Japan.

REFERENCES

Adair E R and Adams B W. 1980 Microwaves modify thermoregulatory behavior in squirrel monkey. Bioelectromagnetics **l** 1-20

Adair E R, Adams B W, Akel G M. 1984 Minimal changes in hypothalamic temperature accompany microwave-induced alteration of thermoregulatory behavior. Bioelectromagnetics **5** 13–30

Adair E R and Black D R. 2003 Thermoregulatory responses to RF energy absorption. Bioelectromagnetics Supplement **6** S17-S38

American Conference of Government Industrial Hygienists (ACGIH) 1996 Threshold limit values for chemical substances and physical agents and biological exposure indices (Cincinnati OH)

ANSI Standard C95.1 1982 Safety levels with respect to human exposure to radio frequency electromagnetic fields, 300kHz to 100GHz

Bernardi P, Cavagnaro M, Pisa S, and Piuzzi E. 2003 Specific absorption rate and temperature elevation in a subject exposed in the far-field of radio-frequency sources operating in the 10-900-MHz range. IEEE Trans Biomed Eng 50: 295-304

Cooper T E and Trezek G J. 1971 Correlation of thermal properties of some human tissue with water content. Aerospace Med. **50** 24-27

D'Andrea J A, DeWitt J R, Gandhi O P, Stensaas S, Lords J L, Neilson H C. 1986 Behavioral and physiological effects of chronic 2450-MHz microwave irradiation of the rat at 0.5 mW/cm^2. Bioelectromagnetics **7** 45-56

Ebert S, Eom S J, Schuderer J, Spostel U, Tillmann T, Dasenbrock C, and Kuster N. 2005 Response, thermal regulatory threshold of restrained RF-exposed mice at 905 MHz. Phys Med Biol **50** 5203-5215

Elder J A and Cahill D F eds., ; 1984 Biological Effects of Radio frequency Radiation, U.S. Environmental Protection Agency, Research Triangle Park. NC27711. Document EPA-600/8-83-026F

Gabriel C. 1996. Compilation of the dielectric properties of body tissues at RF and microwave frequencies. Final Tech Rep Occupational and Environmental Health Directorate. AL/OE-TR-1996-0037 (Brooks Air Force Base, TX: RFR Division).

Gordon RG, Roemer RB, Horvath SM. 1976 A mathematical model of the human temperature regulatory system-Transient cold exposure response. IEEE Trans Biomed Eng **23** 434-444

Hirata A, Watanabe S, Taki M, Kojima M, Hata I, Wake K, Sasaki K, and Shiozawa T. 2006 Computational verification of anesthesia effect on temperature variation in rabbit eyes exposed to 2.45-GHz microwave energy. Bioelectromagnetics **27** 602-612

Hirata A, Asano T, and Fujiwara O. 2007 FDTD analysis of human body-core temperature elevation due to RF far-field energy prescribed in ICNIRP guidelines. Phys Med Biol **52**: 5013-5023

Hobbs B A, Rolhall T G, Sprenkel T L, and Anthony K L. 1991 Comparison of several combinations for anesthesia in rabbits. Am. J. Vet. Res. **52** 669-674

Hoque M and Gandhi O P. 1988 Temperature distribution in the human leg for VLF-VHF exposure at the ANSI recommended safety levels. IEEE Trans Biomed Eng 35: 442-449 IEEE C95.1. 2006 IEEE standard for safety levels with respect to human exposure to radio frequency electromagnetic fields, 3 kHz to 300 GHz. New York: IEEE

International Commission on Non-Ionizing Radiation Protection (ICNIRP). 1998 Guidelines for limiting exposure to time-varying electric, magnetic, and electromagnetic fields (up to 300 GHz). Health Phys **74** 494-522

International Commission on Radiological Protection (ICRP). 1975 Report of the Task Group on Reference Man vol.23, Pergamon Press: Oxford

Kojima M, Hata I, Wake K, Watanabe S, Yamanaka Y, Kamimura Y, Taki M, and Sasaki K. 2004 Influence of anesthesia on ocular effects and temperature in rabbit eyes exposed to microwaves. Bioelectromagentics **25** 228-233

Marai I F M, Habeeb A A M, and Gad A E. 2002 Rabbits' productive, reproductive and physiological performance traits as affected by heat stress: a review. Livestock Prod. Sci. **78** 71-90

Michaelson S M 1983 Biological effects and health hazard of RF and MW energy; fundamentals and overall phenomenology. In: Biological effects and dosimetry of nonionizing radiation (M. Grandolfo, S. M. Michaelson, and A. Rindi, eds.) New York, Plenum Press 337-357

Pennes H H. 1948 Analysis of tissue and arterial blood temperatures in resting forearm. J. Appl. Physiol. **1** 93-122

Samaras T, Christ A, and Kuster N. 2006 Effects of geometry discretization aspects on the numerical solution of the bioheat transfer equation with the FDTD technique. Phys. Med. Biol. **51** 221-229

Shellock F G and Crues J V. ; 1987 Temperature, heart rate, and blood pressure changes associated with clinical imaging at 1.5 T. Radiology **163** 259 –262

Stern S, Margolin L, Weiss B, Lu S, Michaelson S M. Microwaves 1979 effects on thermoregulatory behavior in rats. Science **206**: 198-1201

Taflove A and Brodwin M E. 1975 Computation of the electromagnetic fields and induced temperatures within a model of the microwave-irradiated human eye. IEEE Trans. Microw. Theory Tech **23** 888–896

Taflove A and Hagness S. 1995 Computational Electrodynamics: The Finite-Difference Time-Domain Method: 2nd Ed. Norwood. MA: Artech House

Tuma RF, Irion GL, Vasthare US, Heinel LA. 1985 Age-related changes in regional blood flow in the rat, Am J Physiol **249** H485-H491

Wake K, Hongo H, Watanabe S, Taki M, Kamimura Y, Yamanaka Y, Uno T, Kojima M, Hata I, and Sasaki K. 2007 Development of a 2.45-GHz local exposure system for in vivo study on ocular effects. IEEE Trans Microwave Theory & Tech. **55** 588-596

Wissler E H 1998 Pennes' 1948 paper revisited J Appl. Physiol. **85** 36-42

FIGURE AND TABLE CAPTION

Table 1. Thermal parameters of rabbit tissues.

Figure1. (a) Diagrammatic representation of the exposure system, and (b) its photograph.

Figure 2. Probe positions to estimate an equivalent power density of microwave incident to rabbits.

Figure 3. SAR distributions in the numeric rabbit phantom when exposed to 2.45-GHz plane wave with the power density of 252 W/m^2: (a) bird's eye view and (b) on the cross section across the ear lobe.

Figure 4. Body-core temperature elevation under the condition (a) with and (b) without anesthesia. Calculations with and without thermoregulatory response (TR) are given in case of (b). The power density of microwave was 252 W/m^2.

Figure 5. Temperature elevation in the lens under the condition (a) with and (b) wihtout anesthesia. Calculations with and without thermoregulatory response (TR) are given in case of (b). The power density of microwave was 252 W/m^2.

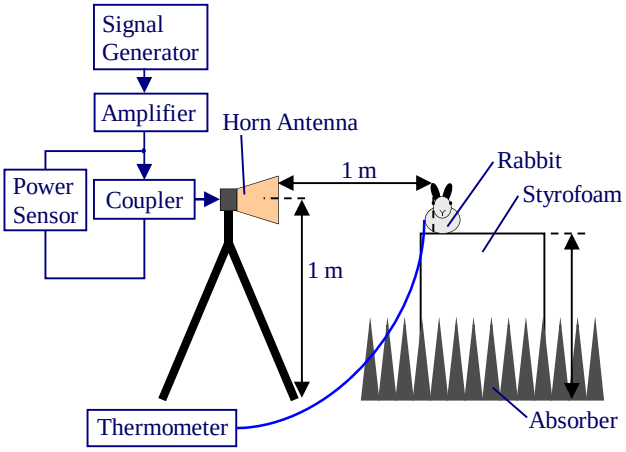

Fig. 1 (a)

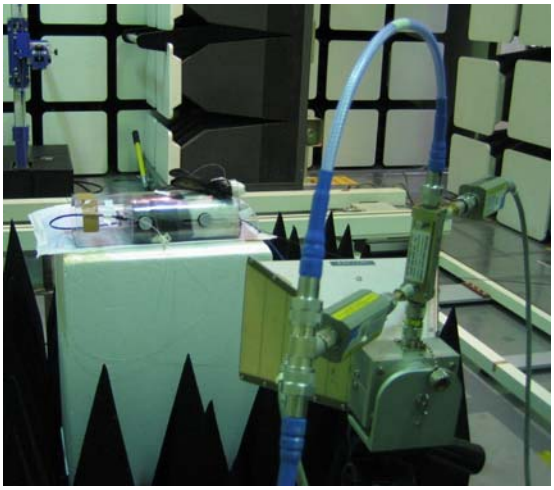

Fig. 1 (b)

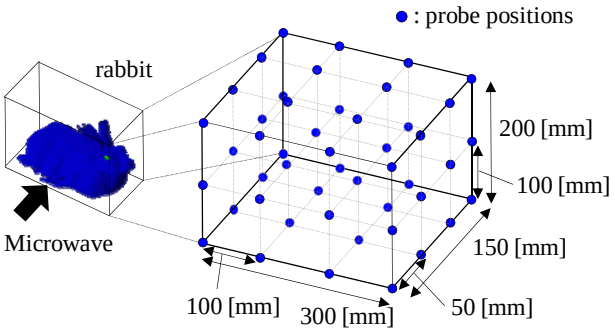

Fig. 2

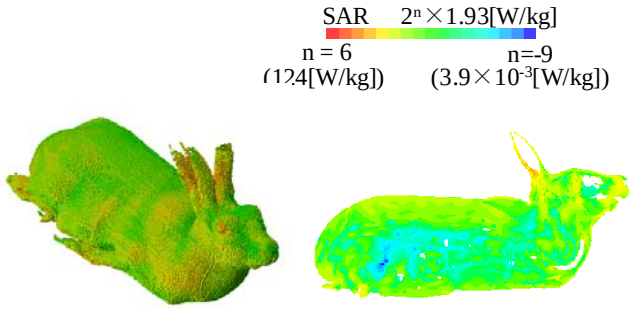

(a) (b)

Fig. 3

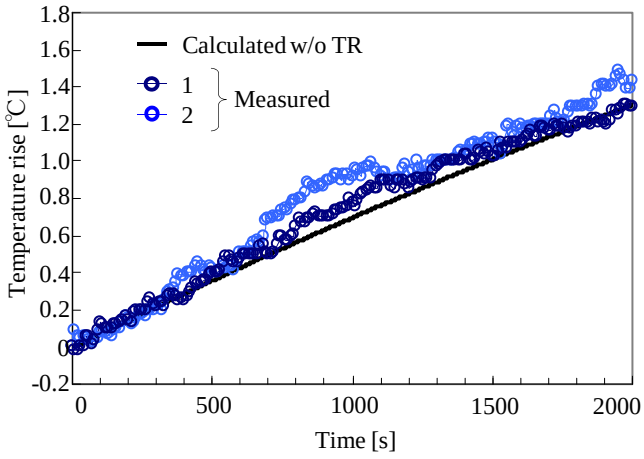

(a)

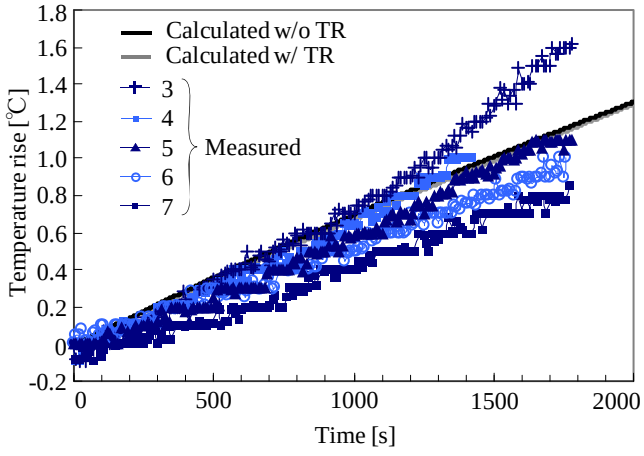

(b)

Fig. 4

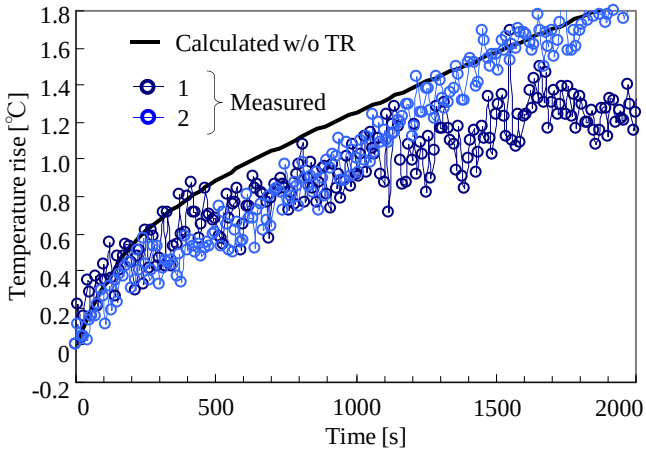
Calculated w/o TR
1
2
Measured
Temperature rise [°C]
Time [s]
1.8
1.6
1.4
1.2
1.0
0.8
0.6
0.4
0.2
0
-0.2
0
500
1000
1500
2000

(a)

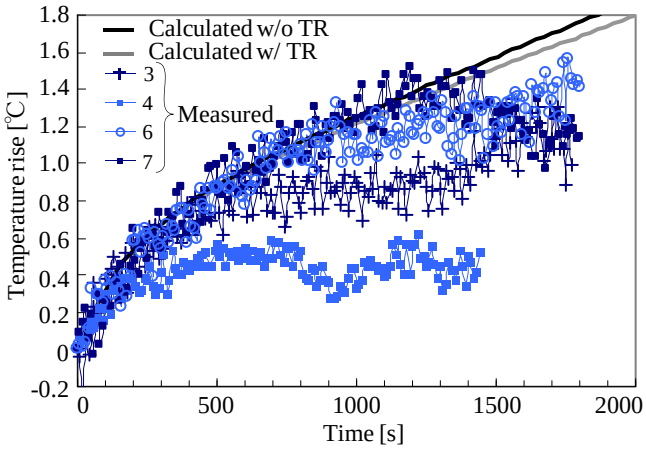
Calculated w/o TR
Calculated w/ TR
3
4
6
7
Measured
Temperature rise [°C]
Time [s]
1.8
1.6
1.4
1.2
1.0
0.8
0.6
0.4
0.2
0
-0.2
0
500
1000
1500
2000

(b)

Fig. 5